Journal of
Materials Chemistry A

Accepted Manuscript

This article can be cited before page numbers have been issued, to do this please use: Y. Jin, J. Chang, Y. Shi, L. Shi, S. Hong and P. Wang, *J. Mater. Chem. A*, 2018, DOI: 10.1039/C8TA00187A.

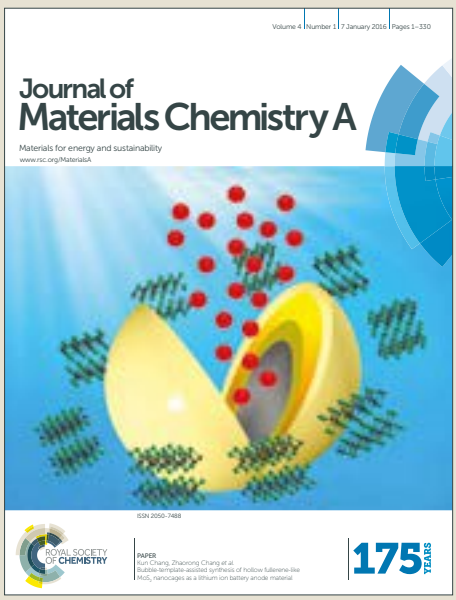

ROYAL SOCIETY OF CHEMISTRY

rsc.li/materials-a

View Article Online
DOI: 10.1039/C8TA00187A

Highly Flexible and Washable Nonwoven Photothermal Cloth for Efficient and Practical Solar Steam Generation

Yong Jin[1#], Jian Chang[1#], Yusuf Shi[1], Le Shi[1], Seunghyun Hong[1], Peng Wang[1,2]*

1. Water Desalination and Reuse Center, Division of Biological and Environmental Science and Engineering, King Abdullah University of Science and Technology, Thuwal, Saudi Arabia, 23955-6900

2. KAUST Solar Center, King Abdullah University of Science and Technology, Thuwal, Saudi Arabia, 23955-6900

*# Both authors contributed equally; *Corresponding author: peng.wang@kaust.edu.sa*

Abstract: Solar-driven water evaporation is emerging as a promising solar-energy utilization process. In the present work, highly stable, flexible and washable nonwoven photothermal cloth is prepared by electrospinning for efficient and durable solar steam evaporation. The cloth is composed of polymeric nanofibers as matrix and inorganic carbon black nanoparticles encapsulated inside the matrix as light absorbing component. The photothermal cloth with an optimized carbon loading shows a desirable underwater black property, absorbing 94% of the solar spectrum and giving rise to a state-of-the-art solar energy utilization efficiency of 83% during pure water evaporation process. Owing to its compositions and special structural design, the cloth possesses anti-photothermal-component-loss property and is highly flexible and mechanically strong, chemically stable in various harsh environment such as strong acid, alkaline, organic solvent and salty water. It can be hand-washed for more than 100 times without degrading its performance and thus offers a potential mechanism for foulant cleaning during practical solar steam generation and distillation processes. The results of this work stimulate more research in durable photothermal materials aiming at real world applications.

Keywords: nylon 6, carbon black, washable, photothermal cloth, water evaporation

View Article Online
DOI: 10.1039/C8TA00187A

1. Introduction

Given the vast abundance and inexhaustibility of sunlight, tapping into solar energy to produce clean water seems a viable solution to current global challenges of water scarcity and energy shortage. [1, 2] Among all possible solar energy utilization methods, solar driven water evaporation, which uses photothermal materials to capture and convert sunlight to heat so to generate water vapor, is quite promising for getting potable water from a variety of source waters.

Thanks to the newly rejuvenated interfacial heating concept[3] and the fast advancement of rational photothermal designs, the solar driven water evaporation efficiency has been significantly improved in the past few years. [4] While the pool of photothermal materials keeps growing, with black titanium oxide, [5-7] MXene, [8] Fe_3O_4, [9, 10] Cu_7S_4, [11] germanium, [12] Al nanoparticles[13] and MoO_{3-x} quantum dots[14] being very recently added into the photothermal material library, the conventional photothermal materials have been well investigated, majorly including such inorganic materials as plasmonic nanoparticles (Ag and Au), [4,15-25] carbon black, [26-28] carbon nanotube, [29,30] graphene based materials, [31-38] *etc.* When designed properly, these conventional materials are capable of producing the state of the art solar to water evaporation efficiency at lab scales, which, to a big extent, disincentives the further search for new photothermal materials.

Therefore, instead of looking for new materials, the challenge facing the solar driven water evaporation is now how to push these lab designs/materials into practical applications. At the status quo, the photothermal materials with good light absorptivity are typically deposited onto substrates with high mechanical strength *via* weak interaction. This configuration unfortunately leads to an easy loss of the photothermal materials to their surroundings in response to external mechanical forces (e.g., abrasion and washing) or due to corrosion in harsh environment，which decreases the lifetime of the photothermal materials and may cause environmental concerns due to the toxicity of these materials. Furthermore, the mechanically strong substrates

View Article Online
DOI: 10.1039/C8TA00187A

are typically inflexible and fragile, which makes them not durable and hard to clean once contaminated or fouled during practical applications. To this end, polymeric photothermal materials, including polypyrrole[39] , polydopamine, [40] and latex [41]have recently been proposed and investigated as a potential solution to provide flexibility. However, the photo-stability and light absorption ability of them are the major obstacles in the way of their practical applications. So far, the choices of water stable, photostable and effective light absorbing polymers are limited and the chemical stability, photo-stability and light-to-heat conversion performance of inorganic photothermal materials are still superior to these of the organic ones.

However, widely available are a variety of chemically stable, mechanically stable, and photostable polymers which have poor light absorptivity (e.g. polyamide, polystyrene, polyacrylonitrile). These polymers, when combined with inorganic photothermal materials, may offer certain potential in presenting chemical, mechanical, photostable, and, at the same time, flexible and durable photothermal materials.

Herein, we rationalize that encapsulating inorganic photothermal material within polymeric fibrous matrix would offer anti-photothermal-material-loss, mechanical strength, structural flexibility, and at the same time, effective photothermal conversion as illustrated in Figure 1a. The composite material, once made, should provide significant advantages in practical applications of solar driven water evaporation.

As a proof of concept, we choose inexpensive carbon black as photothermal material and use electrospinning to encapsulate the carbon black into polymer nanofibers (*e.g.*, nylon 6). The thus-prepared composite photothermal materials in the form of highly flexible and durable nonwoven clothes exhibit an excellent full solar spectrum absorption (>94%) and the state of the art solar driven water evaporation efficiency under one sun irradiation (~83%). Moreover, the clothes are very light, mechanically and chemically stable in various harsh environments and they can be mechanically washed for hundreds times without any degraded photothermal

View Article Online
DOI: 10.1039/C8TA00187A

performance, which the previous photothermal materials fail to do. We believe that the design of the polymeric-inorganic-photothermal composite in this work provides insight towards utilization of photothermal materials towards practical applications.

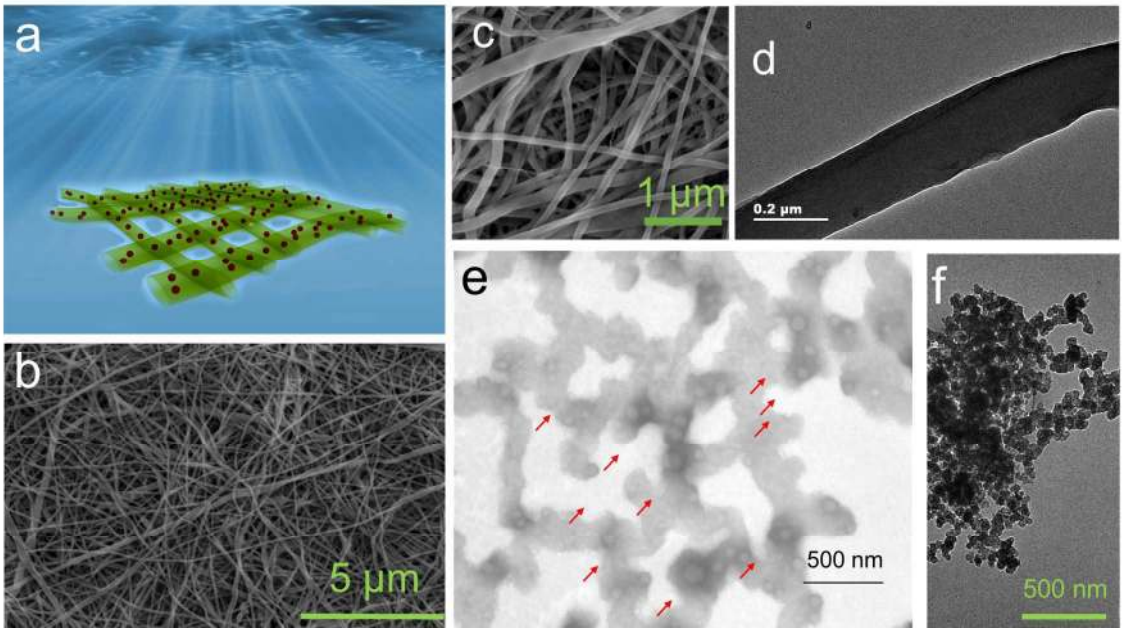

Figure 1. (a) Illustration of the design of the composite photothermal material with inorganic photothermal material encapsulated inside fibrous polymeric matrix; (b) SEM images of the electrospun nylon/carbon cloth, (c) High resolution SEM images of the electrospun nylon/carbon cloth; (d) TEM image of a single nanofiber of the nylon/carbon black fiber; (e) TEM image of nylon/carbon black fiber after being stained with phosphotungstic acid(red arrows indicated carbon black) ; (f) TEM image of the carbon black nanoparticles.

2. Results and Discussions

General design concept, material synthesis and characterizations

In this work, electrospinning is employed to prepare the composite photothermal materials, with nylon 6 (nylon) being polymer matrix and carbon black being photothermal material. Before electrospinning, the carbon black nanoparticles are dispersed uniformly in polymer solution by

View Article Online
DOI: 10.1039/C8TA00187A

ultra-sonication. Aluminum foil substrate is used as the collector and the mass ratio of the carbon black to the polymer is adjusted and optimized.

Figures 1 b presents SEM image of the electrospun composite photothermal materials with 5% mass ratios of carbon black to nylon 6. Clearly, the electrospun material takes on a form of nonwoven cloth composed of stacked individual nanofibers (Figure 1b and Figure S1a). Figure 1c presents the SEM image of nylon-c cloth with a higher magnification, which shows that the diameter of the composite fiber largely ranges from 100 to 400 nm. The SEM images show that the electrospun material is uniformly composed of nanofibers, indicating that there is no phase separation between nylon 6 and carbon black. A closer look at the nylon-c cloth nanofibers under TEM (Figure 1d) reveals rather smooth surface. Till now, it is obvious that carbon black is encapsulated inside the nylon 6 nanofibers. In order to directly observe the encapsulation structure, the fibers are stained with phosphotungstic acid which can react with nylon 6 rather than carbon black. Thus, nylon 6 shows darker than carbon black under TEM. As show in Figure 1e, it is obviously seen that carbon black nanoparticles (lighter round shape indicated by red arrows) are distributed with nylon 6 phase. The size of lighter stains matches well with the size of carbon black directly observed under TEM (Figure 1f, less than 50 nm).

Other polymers such as polyacrylonitrile (PAN) and polystyrene (PS) were also used as polymer matrix for electrospinning. Similarly, the electrospun materials also takes on a form of nonwoven cloth composed of stacked individual nanofibers (Figure S 1b and 1c). However, the mechanical strength of these clothes varies dramatically. The clothes prepared from PAN and PS could be easily tear-broken with a weight of 0.2 kg while the nylon 6 composite cloth shows a much stronger strength under otherwise the same test condition due to the intrinsic mechanical strength of nylon (Figure S 1d). Considering real world application, the cloth of nylon/carbon, denoted as nylon-c thereafter, is then chosen as the candidate for photothermal applications presented in the following sections.

View Article Online
DOI: 10.1039/C8TA00187A

Unique light reflection and absorption properties by nylon/carbon cloth in their wet and dry states

The nylon-c nonwoven cloth shows a very interesting light absorption and reflection transition from their dry to wet conditions. As shown in Figure 2a, the nylon-c clothe (ratio of carbon black to nylon 6: 5%) presents a quite contrasting and interesting coloration comparison in their dry and wet states, namely, when wetted by water. The wet clothes show much darker color, indicating the changes in their light absorption or reflection at least in the visible range. Since the wet conditions are more relevant to the application of photothermal material to water evaporation, the dark black color of the wet composite clothes implies their great light harvesting property.

The light absorption by water in the wet composite photothermal materials can be excluded as a significant contributor to the enhanced light absorption by the wet materials since at least water is transparent across visible light spectrum.

Light travels in different media with different velocities, which can be characterized by the specific refractive index (n) for the light and medium. The refractive index of air, water and nylon 6 are 1.00, 1.33, and 1.53 respectively, presenting a refractive index gradient (Figure 2b). Fresnel equation determines the intensity of electromagnetic waves reflected or transmitted by the interface when electromagnetic waves travel from one medium to another and according to Fresnel equation, the reflectivity (R) is calculated as:

$$R = \left(\frac{n_1 - n_2}{n_1 + n_2}\right)^2 \quad Equation\ 1$$

Where n_1 and n_2 are the refractive index for medium 1 and medium 2. From Equation 1, it can be inferred that adding an intermediate layer whose refractive index is between medium 1 and 2 would reduce the total reflection loss.

View Article Online
DOI: 10.1039/C8TA00187A

In the case of the dry composite photothermal materials, there are air/polymer and polymer/carbon interfaces while in the case of the wet photothermal materials, there are air/water, water/polymer, and polymer/carbon interfaces. From Equation 1, the nylon-c cloth gives rise to $R_{air\text{-}nylon/c}$=4.4% in dry condition while $R_{air\text{-}water\text{-}nylon/c}$=2.5% in wet condition, showing reduced light reflection in wet condition, which well explains the color difference in Figure 2a. It has to be pointed out that this calculation does not consider the incident light angle effect (i.e., assuming 90^o uniformly) and interference between reflected waves and it is just a rough estimation to aid further discussions.

To confirm above analysis, measurements of their light reflection and absorption are conducted. During these measurements, there is no light transmission through the composite clothes and thus the light reflection and adsorption add up to unity. The results show that the light reflection of the wet nylon-c composite in the whole range (i.e., 350 to 2000 nm) is smaller than that of the same composite in dry state for all three carbon to polymer mass ratios (Figure 2c). This is especially true in the visible range (i.e., 400-800nm). As expected, the light absorption of the same materials shows the opposite trend, with much higher light absorption in the wet state than in the dry state (Figure 2d). Similar results are also observed in the cases of the electrospun composite carbon and PAN and PS clothes (Figure S2 and Figure S3).

By comparing different carbon to polymer mass ratios, it seems that the mass ratio of carbon to polymer of 5.0% is an optimal one as further increase to 6.7% does not lead to an obvious benefit of enhanced light absorption (Figure 2c and 2d). Considering the majority of solar irradiation energy lies in the range of 350-2000nm, it is estimated that the wet carbon-polymer would absorb nearly 94% of the total solar energy, which is comparable to the absorption of pure carbon black (around 95%, Figure S4). Thus, our results clearly show that the composite carbon black encapsulated polymeric fibrous clothes have unimpaired and excellent light adsorption property, which is an essential prerequisite to a successful photothermal design.

View Article Online
DOI: 10.1039/C8TA00187A

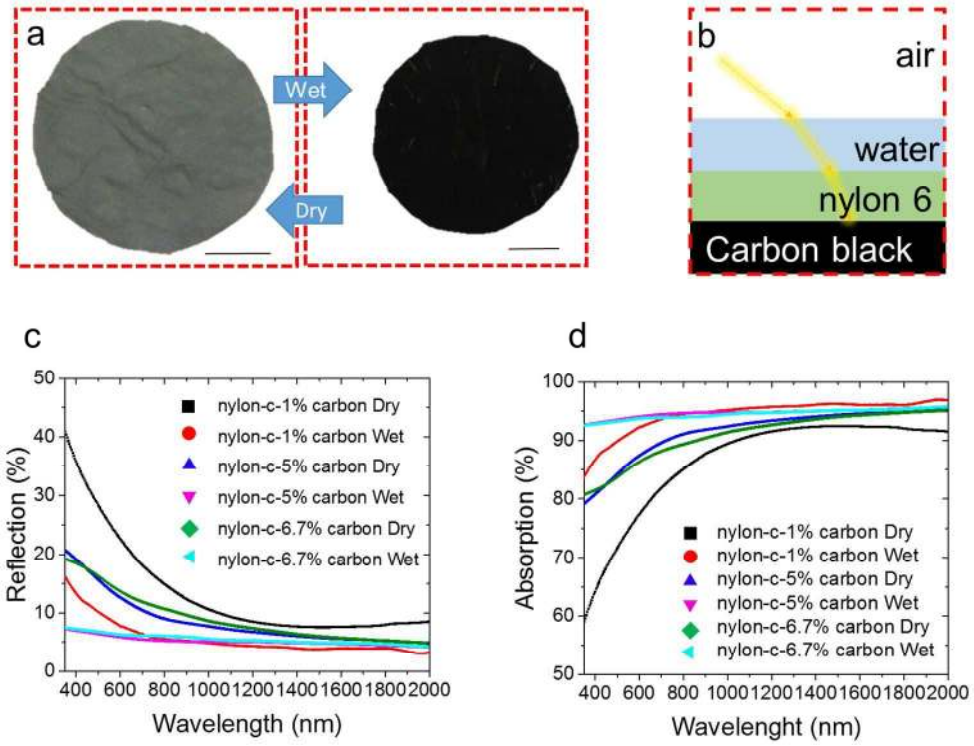

Figure 2. (a) Optical images comparing the colors of the nylon-c (5%) clothes in their dry and wet conditions; scale bar: 1cm; (b) schematic showing refractive index gradient; UV-Vis-NIR (c) reflection and (d) absorption of the nylon-c clothes with different carbon black to nylon 6 ratios in their dry and wet conditions

Moreover, the porous nano-fibrous structures of the electrospun clothes help increase light absorption by creating multiple reflections inside the pores. Thus, the special dry-to-wet light absorption transition property of the composite materials makes the composite possess outstanding light capture ability in spite of the carbon black being embedded inside the polymer in this work.

Mechanical stability, flexibility, chemical durability and thermal stability of the composite cloth

View Article Online
DOI: 10.1039/C8TA00187A

Due to the rationally designed structure and intrinsically excellent mechanical property of nylon 6, the photothermal clothes in this work show some prominent properties which the previous photothermal materials do not possess.

First, the cloth is light in weight because of the low density materials used and high porosity of the clothes. As shown in Figure 3a, the 283 cm^2 dry nylon-c cloth weighs only 0.0627 g. Considering that the thickness of the cloth is around 30 μm (upper panel of Figure 3a), the density of the cloth is only 70 mg cm^{-3}. The light weight of a photothermal material is advantageous for storage and transportation purposes. However, although light, the tensile strength of the nylon-c cloth is high. The maximum tensile stress of the nylon-c cloth is around 17 MPa, which is partially due to the inherent tensile strength of nylon 6 (Figure 3b, red line). It means that the nylon-c cloth with 2 cm width can easily hold 0.2 kg weight as shown in the inset image of Figure 3b. Compared to the original nylon 6 cloth without carbon, the nylon-carbon composite cloth can withstand more energy input (integration of stress over the strain) before breaking. This greater tensile strength of the composite is beneficial for their practical applications. Moreover, the nylon-c cloth is very flexible (Figure 3c) and they can withstand repeated folding and unfolding to their initial state for several hundred times.

Chemical durability is also an important requirement for photothermal materials when they are applied to practical applications during which they may encounter various kinds of harsh conditions. Many previous photothermal materials suffer from poor durability and due to their inherent weak interaction with the matrix materials, the photothermal materials can be easily wiped off their hosting matrix by external forces and be lost permanently. For the purpose of comparison, in this work, the same carbon black nanoparticles are deposited directly onto a filter paper and the durability of the photothermal particles in the filter paper is then compared with that of the nylon-c cloth. Figure 3d compares the scenarios of two materials being sonicated for 5 minutes. Clearly, there are no visible black particles in the water vial of the

View Article Online
DOI: 10.1039/C8TA00187A

nylon-c cloth after the sonication while the aqueous solution in the vial of the carbon and filter paper composite becomes very dark, indicating huge loss of the carbon black particles in the latter case. Figure 3e compares the scenarios of two materials subjected to physical abrasion by finger and presents convincing result of the nylon-c cloth having anti-particle-loss mechanism while the other material has none. The encapsulated carbon particles inside the polymeric matrix in our material guarantees no photothermal component loss during practical applications.

Furthermore, Figure 3f shows the optical and SEM images of the nylon-c cloth being exposed to various chemically harsh conditions (1 M HCl, 1M NaOH, chloroform solvent and 3.5% NaCl solution) for 3 weeks and heat treatment at 100 ºC in 3.5% NaCl solution for 1 week. Due to the inherent chemical stability of nylon 6, the nylon-c cloth survives the harsh conditions, showing no obvious visual and mechanical changes. There are no black particles identified in the solutions after the 3-week treatments in all cases. The SEM images confirm the nanostructure integrity after the treatments (Figure 3f).

Thus, in our design, the selection of nylon 6 as the hosting polymeric matrix and carbon black as light absorbing photothermal component perfectly solves many stability problems that many of the previous materials have. The enhanced mechanical stability, high flexibility, and durability of the nylon-c enable its washability. The nylon-c cloth can be hand washed (Movie S1) and machine washed for many times without showing any structural damages. The washability of the nylon-c cloth enhances its reusability during real life applications where they can be contaminated and fouled.

View Article Online
DOI: 10.1039/C8TA00187A

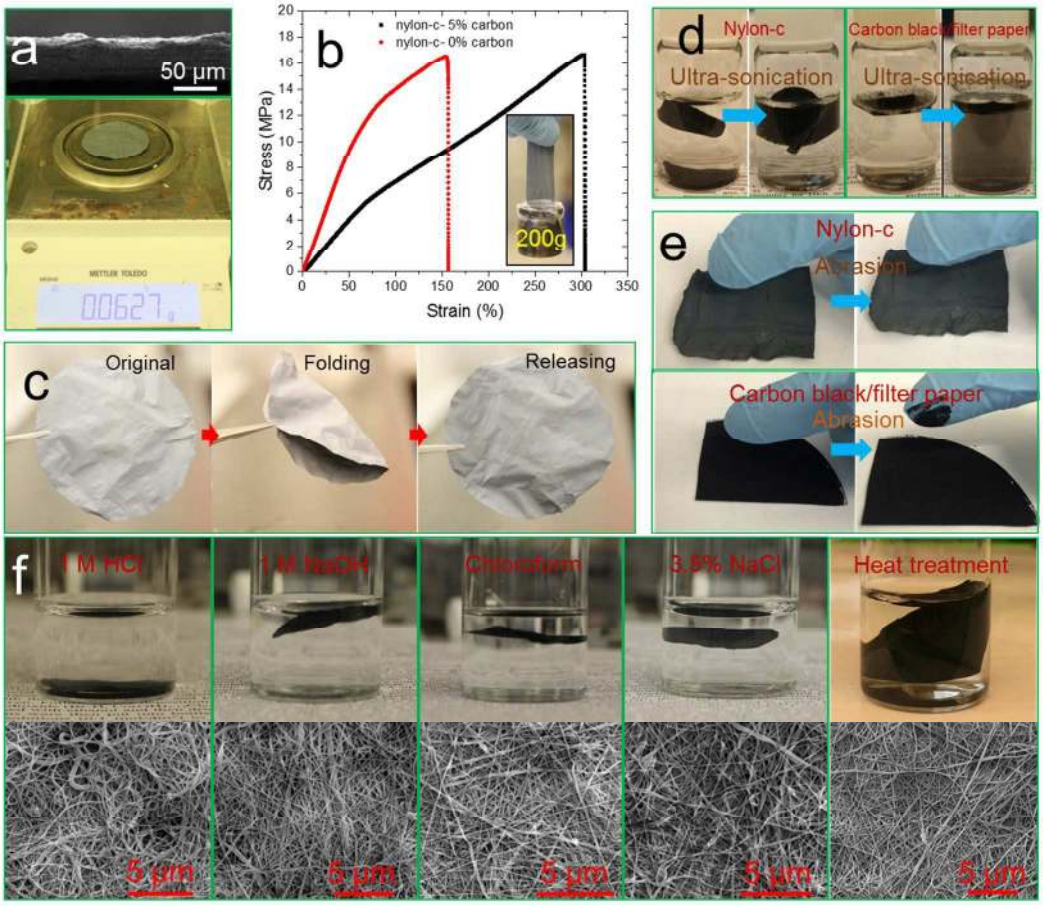

Figure 3. (a) SEM image showing cross section of nylon-c cloth (up) and photo showing the weight of 283 cm^2 nylon-c cloth (down); (b) stress-strain curves of pure nylon 6 cloth and nylon-c dry cloth; (c) photos showing the flexibility of nylon-c cloth; (d) Stability comparison of nylon-c cloth and carbon black/filter paper composite which are sonicated for 5minutes; (e) images showing fingertip abrasion test of nylon-c cloth and carbon black/filter paper composite ; (f) optical and SEM images of nylon-c cloth exposed to 1M HCl, 1M NaOH, chloroform and 3.5% NaCl solutions for 3 weeks and heated at 100 ^{0}C in 3.5% NaCl solution for 1 week.

Photothermal water evaporation test

Given the excellent light absorption performance of the nylon-c cloth, its water evaporation performance is then investigated. Figure 4a presents the schematic solar-driven water evaporation measurement setup in this work. In more details, a solar simulation with an intensity

View Article Online
DOI: 10.1039/C8TA00187A

of 1000 W m^{-2} provides light illumination. The nylon-c cloth is placed on top of a heat barrier of a polystyrene foam with heat conductivity of 0.029- 0.039 W $m^{-1}\cdot K^{-1}$. A small capillary water conduit is provided by using nonwoven cotton cloth to pull water from a bulk water container upwards through a hole in the heat barrier all the way to the photothermal nylon-c cloth. The capillary water conduit easily delivers water to the nylon-c cloth and the water, once there, wets entirely the cloth due to the porous and hydrophilic nature of the nylon-c (Figure S5). The entire system is placed on a digital scale to monitor water evaporation rate of the material continuously and in real time. This design guarantees minimum heat transfer from the photothermal nylon-c cloth layer to the underneath bulk water body. Once the light is on, temperature profiles of the nylon-c clothes with carbon to nylon ratios of 0%, 1%, and 5% are recorded by an infrared camera. Figure 4b shows the optical images and corresponding infrared images under one sun illumination in equilibrium state. From these images, it can be qualitatively concluded that the surface temperature increases with the light absorption of nylon-c cloth increases. Figure 4c gives quantitative surface temperature profile of all nylon-c cloth with different carbon black to nylon 6 ratios.

As seen, all three samples respond to light irradiation rapidly when light is on. Within 100 s, all samples reach their equilibrium temperatures. The equilibrium temperatures of the samples of 0%, 1% and 5% carbon mass ratios are around 27 ºC, 37.3 ºC and 38 ºC, respectively. The equilibrium temperature is a result of energy balance. With input solar flux being fixed, the output energy at equilibrium, including radiation heat loss, convection/conduction heat loss and water evaporation heat loss, is constant and should be equal to the incoming solar flux. All the three energy output means, heat radiation, convection/conduction, and water evaporation are strong functions of the equilibrium temperature.

In our measurement system where the ambient environment is stable with no forced convections, the scenario can be simplified as a horizontal natural convection problem in which

View Article Online
DOI: 10.1039/C8TA00187A

radiation, natural convection and evaporation occur (Figure 4d). In a typical horizontal natural convection scenario, energy balance in the system can be expressed as: [42]

$$\alpha q_{solar} = m_e h_e + \varepsilon\sigma({T_s}^4 - {T_\infty}^4) + h_c(T_s - T_\infty) \quad \text{Equation 2}$$

Where α is the solar absorbance, q_{solar} (W m^{-2}) is the solar energy flux, m_e (g m^{-2} s^{-1}) is water evaporation rate, h_e (J g^{-1}) is latent heat of water evaporation, ε is emissivity of the wet composite, σ is Stefan-Boltzmann constant (5.67 × 10^{-8} W m^{-2} K^{-4}), T_s (K) is wet composite temperature, T_∞ (K) is ambient environment temperature and h_c (W m^{-2} K^{-1}) is convective heat transfer coefficient. Note that heat conduction to bulk water is reasonably neglected due to the design of the evaporation setup.

Based on these analyses, it is identified that the dominant energy loss in our case is the heat radiation due to the low Rayleigh number. (Figure 4d; the more detailed energy analysis and conclusions can be found in the supporting information S6.)

Figure 4e shows the experimental results of pure water evaporation kinetics of the nylon-c clothes under one sun radiation (1000 W m^{-2}). Clearly, the water evaporation rate increases with increasing carbon black amount from 0% to 1% and further to 5%. The evaporation rate for 0%, 1% and 5% are 0.407, 1.22 and 1.24 kg/m^2/h respectively. Based on the water evaporation rates, the energy efficiency, or more accurately, solar-to-water-evaporation efficiency, is then calculated to be 27.7%, 81.4%, 83.1% for the nylon-c clothes with 0%, 1% and 5% carbon black respectively (latent heat of water evaporation at 25 ºC and 40 ºC is 2444 and 2408 KJ kg^{-1} respectively).

More importantly, since the purpose of this work is to produce durable and effective photothermal materials toward long-term and practical applications, we measure the water evaporation rates and further energy efficiency of the nylon-c clothes with 5% carbon black after hand-washing for multiple times and after being treated in various harsh chemical environments.

View Article Online
DOI: 10.1039/C8TA00187A

Figure 4f shows that after 100 hand-washing cycles and being soaked in various harsh environment for 3 weeks, the solar-to-water-evaporation efficiency of the nylon-c cloth remains the same. The fact that these essential performance remains unchanged in all cases agrees with the previous demonstration of the durability of the nylon-c cloth.

The left image in Figure 4g presents a digital photo of the nylon-c cloth being covered by crystallized NaCl salt after 24 hours of solar-driven synthetic seawater (i.e., 3.5% NaCl solution) evaporation using the otherwise the same measurement system. Clearly, the salt deposition on photothermal material is a common occurrence during practical seawater and the deposited salt needs to be cleaned off the photothermal material surface as soon as it affects the light absorption by the material and thus lowers the evaporation efficiency (Figure S7). However, cleaning salt solids off the surfaces of the conventional photothermal materials has been problematic because the physical cleaning, for example, from simple water soaking to sonication, would lead to structural damages and/or photothermal component loss.

The high durability of the nylon-c cloth in this work is made to perfectly fit into salt removal scenario. The right image in Figure 4g presents a digital photo of the previously salt-fouled nylon-c cloth after being hand washed to have the salt deposit removed. The washed nylon-c cloth shows its original black color when wet and the synthetic seawater evaporation rate after washing remains the same (Figure S7)

View Article Online
DOI: 10.1039/C8TA00187A

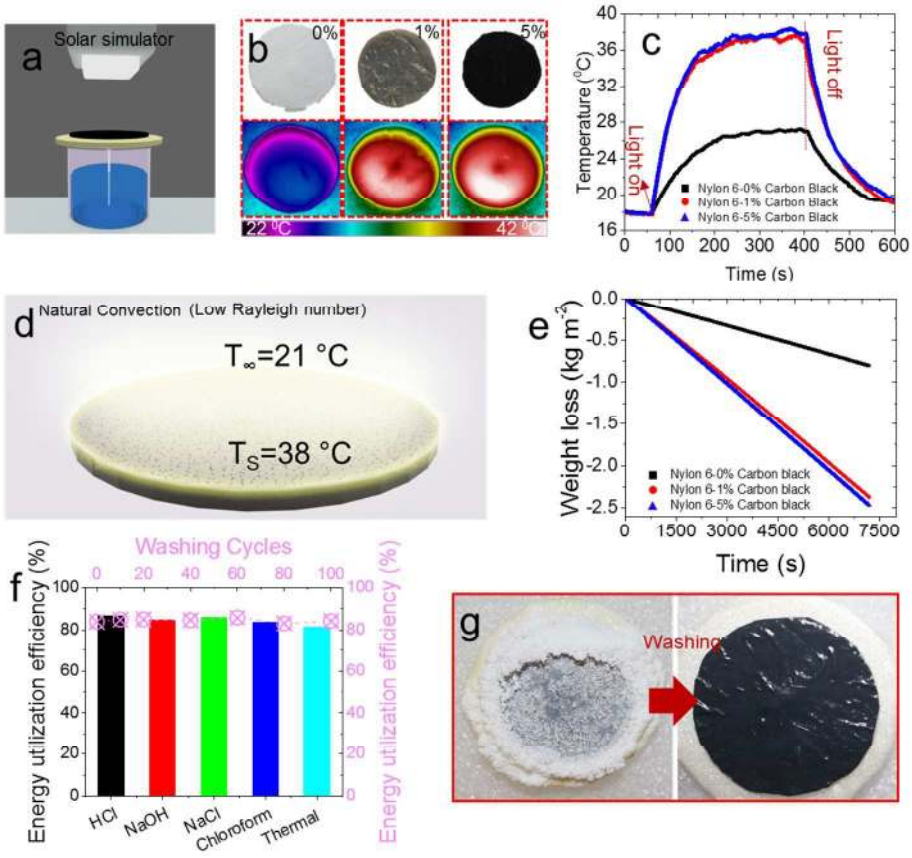

Figure 4. (a) Schematic representation of the water evaporation experimental setup; (b) Optical images and infrared images of nylon-c clothes with different carbon black to nylon 6 ratios (0%, 1%, 5%) under equilibrium states; (c) temperature profiles of the wet photothermal clothes containing 0%, 1% and 5% carbon black; (d) schematic showing the nature convection regime with low Rayleigh number; (e) pure water evaporation kinetics of the clothes (0%, 1% and 5%); (f) solar-to-water-evaporation efficiency of the nylon-c cloth after washing and exposure to various harsh environments; (g) surface solid accumulation after the seawater evaporation (left) and the nylon-c cloth after the salt removal by physically hand washing thoroughly (right).

3. Conclusions

In conclusion, we successfully demonstrate the concept of durable, flexible, washable, and effective nonwoven photothermal cloth by encapsulation of inorganic photothermal material into

View Article Online
DOI: 10.1039/C8TA00187A

polymeric nanofibers. The as-prepared composite photothermal cloth is an excellent light absorber over the solar spectrum. Over 94% of the solar light can be absorbed by the composite material, leading to a solar-to-water-evaporation efficiency of around 83%. Moreover, the photothermal cloth is light, mechanically strong yet durable, chemically and thermally stable in harsh environment. The attractive properties of the photothermal cloth make it a promising material for long-term and practical applications.

4. Methods and Materials

Materials

Nylon 6 pellets, PAN (polyacrylonitrile, MW 150000), PS (polystyrene, MW 192000), DMF (N, N-dimethylformamide, anhydrous, 99.8%) and NaCl (≥98%) were purchased from Sigma-Aldrich. Formic acid (88%) was purchased from Mallinckrodt Baker Chemicals. Carbon black (acetylene, 100% compressed) was purchased from Alfa Aesar. HCl (36.5%-38%) was purchased from Fisher Chemicals. NaOH (≥98%) was purchased from Fluka and chloroform (for HPLC) was purchased from VWR Chemicals. These chemicals were used without further purification.

Preparation of electrospun nonwoven polymer/carbon black cloth

3.0 g nylon 6 pellets were dissolved in 10 ml formic acid, resulting 30% nylon 6 formic acid solution. Different amount of the carbon black (0.03, 0.15 and 0.20 g) was dispersed in the above nylon 6 formic acid solution with the assistance of ultra-sonication, resulting in different ratio of the carbon black to nylon 6 (1.0, 5.0, 6.7%). For PAN, 1.0 g PAN was first dissolved in 10 ml DMF and different amount of the carbon black (0.01, 0.05 and 0.10 g) was dispersed in the above PAN/DMF solution. Similarly, 4.0 g PS was dissolved in 10 ml DMF with different amount of carbon black (0.02, 0.10 and 0.20 g) being added thereafter following the same procedure.

View Article Online
DOI: 10.1039/C8TA00187A

The polymer/carbon black mixture was then electrospun by Esprayer (E-2000s). The electrospinning conditions for nylon 6/carbon black were as follows: applied voltage of 30 kv, the distance between syringe tip and substrate (aluminum foil) of 5.0 cm, and the injection rate of 0.2 ml/h. The electrospinning conditions for PAN/carbon black were: 20kv voltage, 15 cm, and 0.6 ml/h while those of PS/carbon black being 30kv, 15cm, and 1.2 ml/h in the same categories.

Characterizations

Absorption and reflection of UV-Vis-NIR spectrum were obtained with UV-Vis Cary 5000. The data was smoothened in OriginPro 2015 by Savitzky-Golay method (points of window: 50 and polynomial order: 1). SEM images were obtained with Quanta-600 FEI and TEM images were obtained with Tecnai Twin at 120kv. Phosphotungstic acid staining was performed by dissolving phosphotungstic acid in grinded nylon-c cloth water suspension resulting in 1% concentration. Let the suspension stand for 1 min. The tensile strength test was performed by Instron 5942 with a speed of 0.1 mm/s. As a control for the abrasion test, carbon black membrane was prepared by evaporation of ethanol-carbon suspension directly on a filter paper (Whatman, Qualitative 90mm, 100 Circles), which produced carbon-deposited membrane.

Photothermal evaporation experiments

Simulated sunlight (1000 W m^{-2}, Newport Solar 1) perpendicularly irradiated on the photothermal cloth which was placed right on top of an expanded polystyrene heat barrier. The heat barrier was connected with a small capillary water conduit drawing water upwards. The area of the nylon-c composite was around 11 cm^2. Synthetic seawater was prepared by dissolving certain amount of NaCl in DI water, resulting in a concentration of 3.5%. The ambient temperature and humidity were 21 ^{0}C and 60% respectively during the measurements. Temperature profile was recorded by infrared camera (FLIR A655sc) with an emissivity of 0.95 (emissivity of water).

View Article Online
DOI: 10.1039/C8TA00187A

Acknowledgements:

This work was supported by the King Abdullah University of Science and Technology (KAUST) center competitive fund (CCF) awarded to Water Desalination and Reuse Center (WDRC) and KAUST Solar Center (KSC). We thank Professor Frédéric Laquai and Professor Derya Baran from KSC at KAUST for their helpful comments.

References

1 H. Sharon,K.S. Reddy, *Renew. Sust. Energ. Rev.* 2015, **41**,1080-1118.

2 C. M,A. Yadav, Renew. *Sust. Energ. Rev.* 2017, **67**,1308-1330.

3 H. Ghasemi, G. Ni, A.M.Marconnet, J. Loomis, S. Yerci, N. Miljkovic, G. Chen, *Nat. Commun.* 2014, **5**, 4449.

4 G. Liu, J. Xu, K. Wang, *Nano Energy* 2017, **41**,269-284.

5 M. Ye, J. Jia, Z. Wu, C. Qian, R. Chen, P.G. O'Brien, W. Sun, Y. Dong, G.A. Ozin, *Adv. Energy Mater.* 2017, **7**,1601811.

6 J. Wang, Y. Li, L. Deng, N. Wei, Y. Weng, S. Dong, D. Qi, J. Qiu, X. Chen, T. Wu, *Adv. Mater.* 2017, **29**,1603730.

7 L.C. Yi, S.Q. Ci, S.L. Luo, P. Shao, Y. Hou, Z.H. Wen, *Nano Energy* 2017, **41**,600-608.

8 R. Li, L. Zhang, L. Shi, P. Wang, *ACS Nano* 2017, **11**, 3752-3759.

9 Y. Zeng, J. Yao, B.A. Horri, K. Wang, Y. Wu, D. Li, H. Wang, *Energy Environ. Sci.* 2011, **4**, 4074-4078.

10 R. Chen, Z. Wu, T. Zhang, T. Yu, M. Ye, *RSC Adv.* 2017, **7**,19849-19855.

11 C. Zhang, C. Yan, Z. Xue, W. Yu, Y. Xie, T. Wang, *Small* 2016, **12**, 5320-5328.

12 W. Sun, G. Zhong, C. Kübel, A.A. Jelle, C. Qian, L. Wang, M. Ebrahimi, L.M. Reyes, A.S. Helmy, G.A. Ozin, *Angew. Chem. Int. Ed.* 2017, **56**,6329-6334.

13 L. Zhou, Y. Tan, J. Wang, W. Xu, Y. Yuan, W. Cai, S. Zhu, J. Zhu, *Nat. Photon.* 2016, **10**,393-398.

View Article Online
DOI: 10.1039/C8TA00187A

14 D. Ding, W. Huang, C. Song, M. Yan, C. Guo, S. Liu, *Chem. Commun.* 2017, **53**, 6744-6747.

15 Y. Liu, S. Yu, R. Feng, A. Bernard, Y. Liu, Y. Zhang, H. Duan, W. Shang, P. Tao, C. Song, T. Deng, *Adv. Mater.* 2015, **27**,2768-2774.

16 O. Neumann, C. Feronti, A.D. Neumann, A. Dong, K. Schell, B. Lu, E. Kim, M. Quinn, S. Thompson, N. Grady, P. Nordlander, M. Oden, N.J. Halas, *Proc. Natl. Acad. Sci. U.S.A.* 2013, **110**,11677-11681.

17 O. Neumann, A.D. Neumann, E. Silva, C. Ayala-Orozco, S. Tian, P. Nordlander, N.J. Halas, *Nano Lett.* 2015, **15**,7880-7885.

18 O. Neumann, A.S. Urban, J. Day, S. Lal, P. Nordlander, N.J. Halas, *ACS Nano* 2013, **7**,42-49.

19 X. Wang, Y. He, X. Liu, G. Cheng, J. Zhu, *Appl. Energy* 2017, **195**,414-425.

20 L. Zhou, S. Zhuang, C. He, Y. Tan, Z. Wang, J. Zhu, *Nano Energy* 2017, **32**,195-200.

21 M. Zhu, Y. Li, F. Chen, X. Zhu, J. Dai, Y. Li, Z. Yang, X. Yan, J. Song, Y. Wang, E. Hitz, W. Luo, M. Lu, B. Yang, L. Hu, *Adv. Energy Mater.* 2017,1701028.

22 Z. Wang, Y. Liu, P. Tao, Q. Shen, N. Yi, F. Zhang, Q. Liu, C. Song, D. Zhang, W. Shang, T. Deng, *Small* 2014, **10**, 3234-3239.

23 M. Gao, P.K.N. Connor, G.W. Ho, *Energy Environ. Sci.* 2016, **9**,3151-3160.

24 C. Liu, J. Huang, C.-E. Hsiung, Y. Tian, J. Wang, Y. Han, A. Fratalocchi, *Adv. Sustain. Syst.* 2017, 1,1600013.

25 K.Bae, G. Kang, S.K. Cho, W.Park, K. Kim, W.J. Padilla, *Nat. Commun.* 2015, **6**,10103.

26 Y. Liu, J. Chen, D. Guo, M. Cao, L. Jiang, *ACS Appl. Mater. Interfaces* 2015, **7**,13645-13652.

27 P.D. Dongare, A. Alabastri, S. Pedersen, K.R. Zodrow, N.J. Hogan, O. Neumann, J. Wu, T. Wang, A. Deshmukh, M. Elimelech, Q. Li, P. Nordlander, N.J. Halas, *Proc. Natl. Acad. Sci. U.S.A.* 2017, **114**, 6936-6941.

28 N. Xu, X. Hu, W. Xu, X. Li, L. Zhou, S. Zhu, J. Zhu, *Adv. Mater.* 2017, **29**,1606762.

29 Y. Wang, L. Zhang, P. Wang, *ACS Sustain. Chem. Eng.* 2016, **4**,1223-1230.

View Article Online
DOI: 10.1039/C8TA00187A

30 C. Chen, Y. Li, J. Song, Z. Yang, Y. Kuang, E. Hitz, C. Jia, A. Gong, F. Jiang, J.Y. Zhu, B. Yang, J. Xie, L. Hu, *Adv. Mater.* 2017, **29**,1701756.

31 Q. Jiang, L. Tian, K.-K. Liu, S. Tadepalli, R. Raliya, P. Biswas, R.R. Naik, S. Singamaneni, *Adv. Mater.* 2016, **28**, 9400-9407.

32 Y. Li, T. Gao, Z. Yang, C. Chen, W. Luo, J. Song, E. Hitz, C. Jia, Y. Zhou, B. Liu, B. Yang, L. Hu, *Adv. Mater.* 2017, **29**,1700981.

33 L. Shi, Y. Wang, L. Zhang, P. Wang, *J. Mater. Chem. A* 2017, **5**, 16212-16219.

34 K.-K. Liu, Q. Jiang, S. Tadepalli, R. Raliya, P. Biswas, R.R. Naik, S. Singamaneni, *ACS Appl. Mater. Interfaces* 2017, **9**,7675-7681.

35 Y. Ito, Y. Tanabe, J. Han, T. Fujita, K. Tanigaki, M. Chen, *Advanced Materials* 2015, **27**, 4302-4307.

36 P. Zhang, J. Li, L. Lv, Y. Zhao, L. Qu, *ACS Nano* 2017, **11**, 5087-5093.

37 X. Li, W. Xu, M. Tang, L. Zhou, B. Zhu, S. Zhu, J. Zhu, *Proc. Natl. Acad. Sci. U.S.A.* 2016, **113**,13953-13958.

38 Z. Wang, Q. Ye, X. Liang, J. Xu, C. Chang, C. Song, W. Shang, J. Wu, P. Tao, T. Deng, *J. Mater. Chem. A* 2017, **5**,16359-16368.

39 L. Zhang, B. Tang, J. Wu, R. Li, P. Wang, *Adv. Mater.* 2015, **27**,4889-4894.

40 X. Wu, G.Y. Chen, W. Zhang, X. Liu, H. Xu, *Adv. Sustain. Syst.* 2017, **1**,1700046.

41 V. Kashyap, A. Al-Bayati, S.M. Sajadi, P. Irajizad, S. Wang and H. Ghasemi, *J. Mater. Chem. A*, 2017,**5**, 15227-15234

42 G. Ni, G. Li, Svetlana V. Boriskina, H. Li, W. Yang, T. Zhang, G. Chen, *Nat. Energy* 2016, **1**,16126.

View Article Online
DOI: 10.1039/C8TA00187A

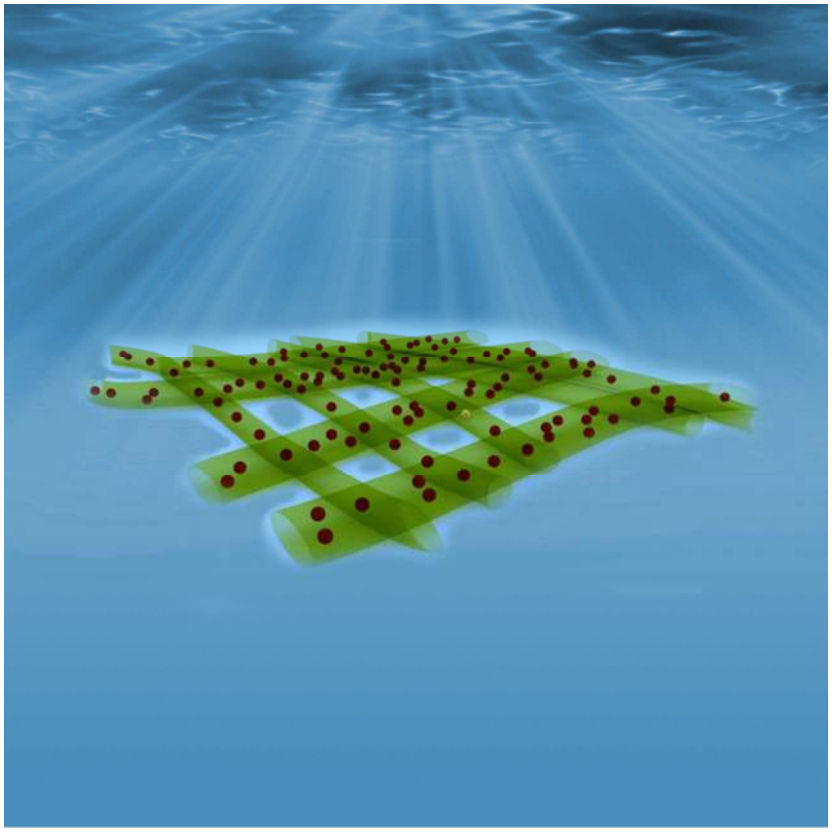

Encapsulating carbon black into nylon 6 matrix makes robust photothermal cloth for highly efficient solar vapor generation